https://doi.org/10.26525/jtfs2022.34.2.236

MECHANICAL AND COLOUR PROPERTIES OF RUBBERWOOD BASED ON THE VARIATION IN WOOD SHRINKAGE

Thanate R[1,] *, Santi K[2] & Chayut N[3]

[1]*Department of Industrial and Manufacturing Engineering, Faculty of Engineering, Prince of Songkla University, Hat Yai, Songkhla 90112, Thailand*
[2]*Faculty of Industrial Technology, Nakhon Si Thammarat Rajabhat University, Nakhon Si Thammarat 80280, Thailand*
[3]*Department of Mechanical and Mechatronics Engineering, Faculty of Engineering, Prince of Songkla University, Hat Yai, Songkhla 90112, Thailand*

**thanate.r@psu.ac.th*

Submitted June 2021; accepted August 2021

Defects in rubberwood is a major problem in the rubberwood industry of Thailand. It was detected during the drying process of rubberwood which caused bow and crook deformations. The current study presented a model that described the change in the magnitude of bow and crook between two moisture contents below the fiber saturation point. The longitudinal shrinkage in the experimental samples was obtained at the moisture content range from 16% to 8%. The model showed that the variation in longitudinal shrinkage coefficient over the cross-section and along the sample could explain most of the changes in bow and crook of the lumber. In addition, it was possible to identify evenly-curved bow and crook. The least value of root mean square error was at 0.115 and standard error of 0.130 for sample 3A1 and root mean square error of 0.179 and standard error at 0.202 for sample 7B3 indicated that these samples had the best model predictions. The model was able to predict the changes in bow better than the changes in crook. Both mechanical and colour properties were comparable to the work of others.

Keywords: distortion, moisture content, rubberwood, multiple linear regression, model prediction

INTRODUCTION

Drying defects is a major problem in wood-related industries which significantly impacted the effective and efficient use of wood products in many countries (Chang et al. 2020, Monteiro et al. 2020, Khamtree et al. 2021). Different drying schedules and techniques were used for different wood species and raw material resources were also becoming less available to the industries. Older trees with large diameters were no longer easily available and younger trees with small diameters, including trees grown on plantations were used as raw materials in several countries. However, timber from these young trees had longitudinal shrinkage which caused deformations of the wood products (Peng et al. 2013, Cáceres et al. 2018). Therefore, the appearance of bows, crooks and twists in softwood structural lumber was a crucial problem to be addressed.

Several methods were currently in commercial use to eliminate the deformations in these products. In fact, the restraint methods which involved high-temperature drying was used because of its maximum effectiveness. High temperatures increased the relaxation of stress before the restraint was released. Consequently, wooden boards treated in this way were less likely to deform. Generally, when the moisture content in wood was less than 30%, the structure began to shrink. The cross-grain shrinkage that occurred was anisotropic in nature, meaning that the radial shrinkage from the pith to the bark of the tree and the tangential shrinkage at the tangent to the annual rings were unequal. The directional or anisotropic nature of cross-grain shrinkage caused distortions in dried wood which resulted in cupped lumber. The word cupped was defined as a distortion of a board in which there was deviation from flatness across the width of the board. The Forest Service Wood Handbook published by the U.S. Department of Agriculture (USDA) provided the average total percent of radial and tangential shrinkage for their domestic and some foreign woods with moisture content in the range from 0% to 30%

(Ross & Service 2010). The Handbook presented an equation that could be used to calculate an estimate of the expected dimensional changes based on the total radial and tangential shrinkage as the moisture in the lumber decreased or increased. The problem of distortions in the wood shape was caused by the internal moisture content evacuating to the surface in the non-equilibrium conditions during drying. The bow and crook deformations were also sensitive to variations in the stiffness properties and the angle of the spiral grain, which might have significant influence on the bowing occurrence (Ormarsson & Cown 2005). Both the shrinkage intersection points and the end of the capillary water values increased with temperature and no distinction between the two values could be made at all times (Lazarescu et al. 2009). The resulting shrinkage was measured by pairs of resistive transducers that were placed at the middle part of each specimen (Lazarescu et al. 2010). Many researchers applied stochastic analysis to explain the distribution field of moisture and its standard deviation, as well as at different drying times and points inside the lumber. Such information was vital for determining the type of uncertainties that existed, to quantify them, and to analyse the drying process a more reliable way (Cermak & Trcala 2012). In addition, twist was another type of distortion in wood shape that must be studied. It was thought that at the time which the timber began to be twisted during drying was subjected to the variation in the radial direction of the grain angle. In other words, timber began to twist when the portion with a large grain angle began to dry. There were concerns that timber with a large grain angle in the inner portion might become twisted during storage after kiln drying (Kubojima et al. 2013).

Therefore, the objectives of the study were to show the relationship between variations in the longitudinal shrinkage coefficient and moisture-induced bowing and crooking and to develop a model that showed the relationship between variations in the longitudinal shrinkage coefficient and moisture-induced bowing and crooking. In addition, the mechanical properties and colour of Eucalyptus and Fagus sylvatica woods had decreased according to the effect of thermally modified process (González-Peña & Hale 2009, Calonego et al. 2012). Thus, the samples were measured and investigated to validate the wood quality.

MATERIALS AND METHODS

Wood sample

Rubberwood samples without any defects such as black knots and lines, cracks, fungus, blue stains, bucks and cores were obtained from a wood factory in Songkhla Province, Thailand. Eighty-one samples were dried in each run. The samples were 76 mm wide, 25 mm thick and 1,150 mm long. Prior to drying, the samples were protected from fungi with a borax-based chemical solution (Ratanawilai et al. 2015). The initial moisture content of dry basis lumber was approximately 40–70%.

Drying process

The laboratory-scale drying chamber was designed to fit samples of typical sizes generally used for the furniture industry. The chamber had an inside width of 600 mm, 200 mm tall and 1,500 mm long (Khamtree et al. 2019). The hot-air drying unit with a temperature controller consisted of a blower, a 3-kW electric heater and a valve. The blower had an inverter that was used to control the velocity of the flow and was connected to an electric heater with a uniform flow filter. A data logger then recorded the measurements provided by the pressure transducer. The weight loss was measured by using a load cell and a K-type thermocouple to measure the temperatures.

The temperature profiles and drying rates of three samples were observed. Sensors were installed inside each sample to measure the gas pressure at three locations along the length of the sample. The drying conditions used in the experiment were wet-bulb temperatures in the range of 40–80 °C. The dry-bulb temperatures were in the range of 80–120 °C of the control system to evaporate the moisture content on dry basis (Simpson 1991, Walker 2006). The airflow was measured using an anemometer in order to control moisture evaporated. The internal and external temperatures in the rubberwood were detected by K-type thermocouples and recorded with a data logger. After the drying process was complete, the sample was extracted from the chamber and the deformations were measured with a ruler and a pair of digital Vernier callipers with ± 1% precision according to European Standards EN 14081-1, EN 518 and EN 519 (Roblot et al. 2008).

Measurement of shrinkage, bow and crook

Selected lumber was used and the comparisons between variations in longitudinal shrinkage, bow and crook were made separately for each sample. After the deformation measurement, a total of 81 samples were sawn into blocks with dimensions of 50 mm × 75 mm × 100 mm. These blocks were then sawn into smaller specimens with dimensions of 25 mm × 25 mm × 60 mm (Figure 1). The samples for this study consisted of 243 tests wood. A total of 81 lumber boards were used to obtain a huge variation in the bow and crook measurement and for the compression of wood content (Johansson 2003). The measurements for weight and length of each sample were recorded while the samples reached an equilibrium moisture content from 90% to 30% relative humidity and at temperature of 20 ± 2 °C (Sik et al. 2010). The oven-dried weight of each sample also was recorded after 24 hours at 103 ± 2 °C. Longitudinal shrinkage was converted to a shrinkage coefficient l, defined as shrinkage strain in percent per percentage moisture content difference using Equation 1 and Equation 2.

$$\varepsilon = \frac{l_1 - l_2}{l_1} \times 100 \qquad (1)$$

$$\alpha_1 = \frac{\varepsilon_1}{u_1 - u_2} \qquad (2)$$

where ε_1 = the shrinkage strain, l_1 = the length at 90% relative humidity, l_2 = the length at 30% relative humidity, α_1 = the longitudinal shrinkage coefficient, u_1 = the moisture content at 90% relative humidity and u_2 = the moisture content at 30% relative humidity (Johansson 2003, Kliger et al. 2003).

Multiple linear regression was a statistical technique used to forecast the greatest relationship between a dependent variable and several independent variables (Tiryaki & Aydın 2014, Bao & Liu 2007). The dependent variables sometimes were named the predictand, and the independent variables were called the predictors. Multiple linear regression was based on the least squares technique, i.e., the model was fit to minimize the sum of squares of the errors between measured and predicted values. In addition, the normal probability plot and residual plot were assessed when fitting a model. The multiple linear regression analysis was conducted using statistics software. In fact, the multiple linear regression model was represented as:

$$Y = ß_0 + ß_1 X_1 + ... + ß_n X_n + \alpha_1 \qquad (3)$$

where Y = the dependent variable, X_i = the independent variables, $ß_i$ = the fitted parameters, and α_1 = the longitudinal shrinkage coefficient.

After the optimum condition was obtained, the samples were dried in a drying cabinet at 65% relative humidity and at 20 ± 2 °C (Altgen & Militz 2016). Prior to the testing, the boards were cut into appropriate dimensions according to the standards. Then wood samples were subjected to mechanical testing including compression and bending tests by ASTM D143 and BS373 standard (Table 1) (Kaung & Thanate 2020).

Colour was one of the subjectively used quality measures of rubberwood and the brightness of the wood could be used to assign it

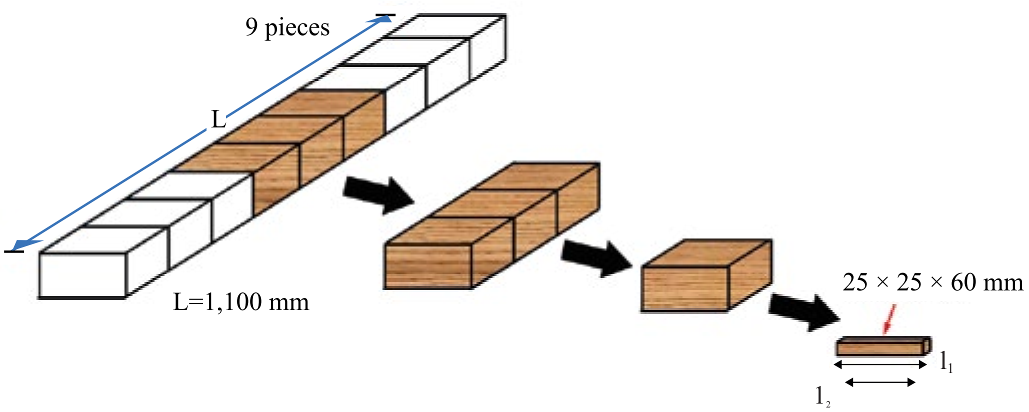

Figure 1 Cutting wood samples into blocks and specimens

Table 1 Standard tests for wood mechanical properties of the samples

Property	Standards for wood test
Compressive stress	
Parallel to grain	ASTM D143 (ASTM D143-14 2014)
Perpendicular to grain	ASTM D143 (ASTM D143-14 2014)
Static bending	BS 373 (Staff & Institution 1957)

a grade. Blue staining of the rubberwood became obvious during the final phases of drying and the total lightness of the specimens decreased with drying time. The effects of the drying conditions on colour were measured by using a colour–difference meter. The time traces of colour were monitored during drying. In order to obtain the total colour variation during the entire drying period, the average core lightness for the specimen was deducted from the average surface lightness for the completely dried sample in the 100 % dried samples. The standard of colour measurement was computed by CIE Lab Scale (Hadi et al. 2020). The measurement was duplicated for the colour coordinates a and b. Subsequently ΔE was determined from these values as shown in Equation 4 to obtain the total difference in colour (Ratnasingam & Grohmann 2014).

$$\Delta E = \sqrt{\Delta L^2 + \Delta a^2 + \Delta b^2} \quad (4)$$

where, ΔE= the colour difference, ΔL= the lightness difference, Δa = the red-green difference and Δb = blue-yellow difference.

RESULTS AND DISSUSION

Measurements of bow and crook

The bow and crook in the middle of the 81 samples for both wet and dry conditions were shown in Table 2. The middle deflection was not always the maximum deflection, but it gave an estimate of deformation that was easy to compare with the deformation values permitted in timber that was used for construction. It also produced a value that could be compared with the predicted deformation. For most of the samples, absolute values of the deformation increased during a change in moisture content. The magnitudes of the changes varied in deviation distance from 5 mm to 16 mm for bow and from 3.2 mm to 12 mm for crook as shown in Table 3. These results matched well the results provided in previous studies (Johansson 2003, Kliger et al. 2003) in which the change in bow was always greater than the change in crook. Figure 2 shows the deviation distances that were measured by the positions on the lumber (100–600 mm) and 600 mm.

Table 2 Bow and crook values recorded at the center of the samples

Run no.	Bow (mm)		Crook (mm)	
	Fresh (Initial MC)	Dry (Final MC)	Fresh (Initial MC)	Dry (Final MC)
1B3	1.3	8.4	1.1	4.3
2A2	2	10	6	17
3A1	2	7	1	6
4C2	1	7	2	8
5C1	2	8	2	9
6B2	2	7	1	5
7B3	2	9	1	13
8A1	2	18	1	6
9A3	2	7	8	19

First digits (1–9) denoted the run numbers of the experiments, A = first row samples, B = second row samples, C = third row samples, third digit (1–3) = the sample number of the wood; MC = moisture content

Table 3 Summary of the measured and predicted differentials in bow and crook at two measured conditions

Run no.	ΔBow (measured) (mm)	ΔBow (predicted) (mm)	ΔCrook (measured) (mm)	ΔCrook (predicted) (mm)
1B3	7.1	6.1	3.2	5.5
2A2	8.0	9.3	11.0	7.2
3A1	5.0	5.4	5.0	5.0
4C2	6.0	6.2	6.0	5.9
5C1	6.0	5.3	6.0	6.1
6B2	5.0	4.3	4.0	4.0
7B3	7.0	7.2	12.0	6.3
8A1	16.0	11.1	5.0	8.7
9A3	5.0	7.8	11.0	6.8

First digits (1–9) denoted the run numbers of the experiments, A = first row samples, B = second row samples, C = third row samples, third digit (1–3) = the sample number of the wood

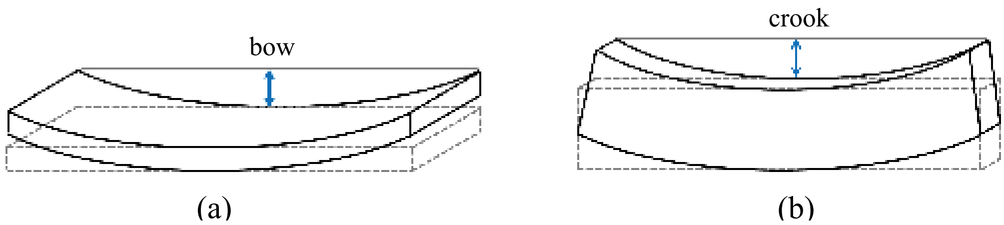

Figure 2 Wood defects in (a) bow and (b) crook

Predicting bow and crook with multiple regression

Based on Equation 3 above, multiple linear regression was used to further analyse the deformation of the wood by position on the sample, the value of the fresh moisture content, the final moisture content and the shrinkage coefficient. Those factors were subjected to tensile or compressive stress that was caused by wood shrinkage. The multiple linear regression analysis on similar data was obtained using the multiple linear regression model, as shown in Equation 5 and Equation 6.

$$Y_{Bow} = -1.48 + 0.000477X_1 + 0.0118X_2 + 0.0139X_3 + 29.3\,\alpha_1 \quad (5)$$

$$Y_{Crook} = -10.8 + 0.000708X_1 - 0.162X_2 - 0.044\,X_3 + 28.1\,\alpha_1 \quad (6)$$

where, X_1 = the position of the samples, X_2, = the fresh moisture content from Table 2, X_3 = the final moisture content from Table 2 and α_l = the shrinkage coefficient.

For model adequacy checking, the studentised residuals h_{ii} must fall in the interval $0 < h_{ii} < 1$. Therefore, the h_{ii} of the multiple linear regression in this study was in the interval including the matrix scatter plot that implied the acceptance of the multiple linear regression. Moreover, Figure 3(a) was the normal probability plot of the residuals and Figure 4(b) was the plot of the residuals versus the predicted values. These plots did not suggest any problems with the assumptions made in the model. Therefore, the regression fits to wood distortion were reasonable and accepted in this study.

Comparison of the experimental and model results

The model was used to assess the changes in the magnitude of bow and crook for two different moisture contents. The change in the magnitude of bow between the two moisture contents was called Δbow, and the change in crook was called Δcrook. The modeled Δbow showed good

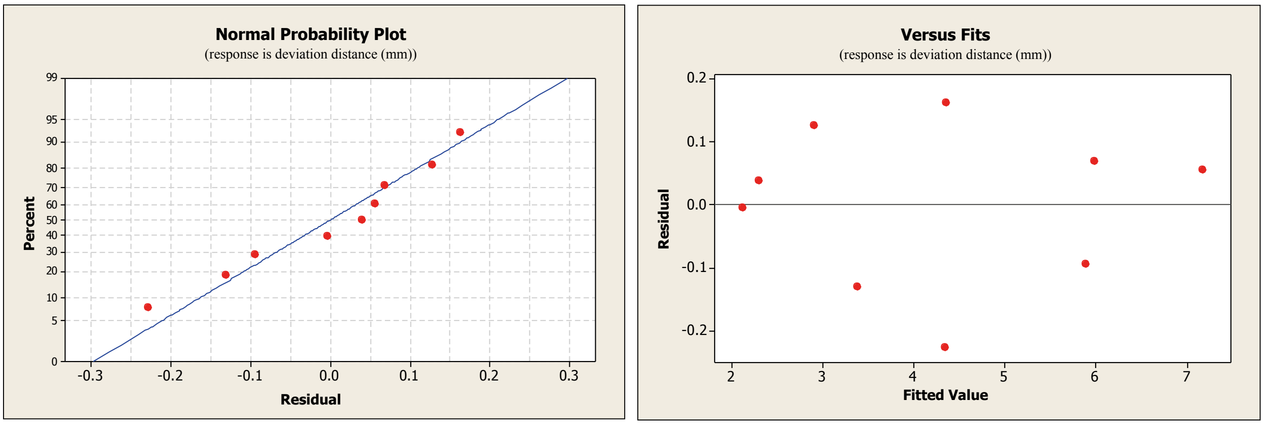

(a) (b)

Figure 3 Normal probability (a) and residual plot (b) of bow regression

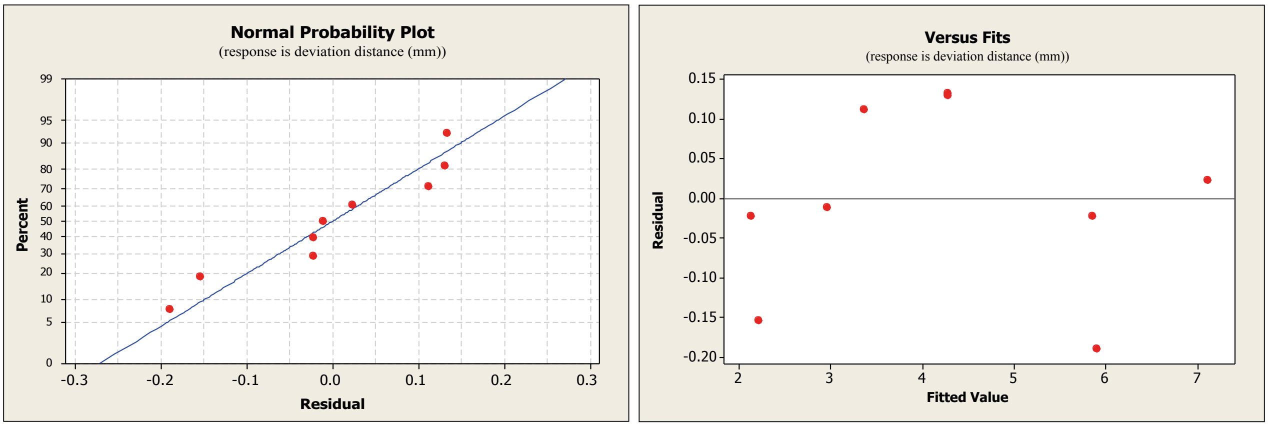

(a) (b)

Figure 4 Normal probability (a) and residual plot (b) of crook regression

agreement with the measured Δbow when the change in the moisture content in the model was set at 8%. The agreement between the measured Δcrook and the predicted Δcrook was not as good as it was for Δbow. The relationship between the measured Δcrook and predicted Δcrook was reasonably good for 7 of the 81 samples. The worse agreement for some boards might be due to samples with knots or uneven compression wood causing the sample to be unrecorded and was not included in the model. Table 3 provided a summary of all of the results i.e., the measured and predicted Δbow and Δcrook at the midpoint of each lumber. The results generally showed good agreement between the measured and predicted values. The observation indicated that the known variation in longitudinal shrinkage coefficient was sufficient to model Δbow and Δcrook with reasonable accuracy. The differences in longitudinal shrinkage from lumber 7B3 and 3A1 were shown in Figures 5(a) and 5(b). Figure 6 showed results for samples 7B3 and 3A1, which displayed the best fit between the measured and predicted values of Δbow and Δcrook. The least values of root mean square error at 0.115 and standard error at 0.130 for sample 3A1 and root mean square error at 0.179 and standard error at 0.202 for sample 7B3 indicated these cases were the best matches with model predictions. By using the model, it was possible to capture the charasteristics of Δbow and Δcrook with good agreement, as was seen in Figure 5(a) and Figure 5(b).

Mechanical properties of the samples

The mechanical properties were measured with reference to the standards in Table 1 for three replications in each test and the results were shown in Table 5. The findings showed compression parallel to the grain to determine the stress of wood after drying at 80 °C was smaller than after drying at 100 °C or 120 °C was acceptable (Figure 7(a) & Figure(b)). A previous study by Sik et al. (2009) has suggested that high temperature drying improved the mechanical properties of rubberwood. The values in Table 4 represented the standard deviation of longitudinal shrinkage. Meanwhile, Table 5 shows the values of compression parallel to grain and the modulus of elasticity of rubberwood. The mechanical properties were in the range of 38.16–40.75 MPa and 7838.35–8679.38 MPa, respectively. These results were consistent with previous works, in which the compression parallel to grain of rubberwood was between 26.6–53.5 MPa (Matan & Kyokong 2003) and 37.10–52.66 MPa (Yamsaengsung & Tabtiang 2011). Moreover, the modulus of elasticity was between 3500–5600 MPa (Matan & Kyokong 2003) and 7388–12678 MPa (Yamsaengsung & Tabtiang 2011). In addition, the modulus of elasticity for rubberwood in Malaysia and India were in the range of 6070–15670 MPa (Gnanaharan & Dhamodaran 1993). Therefore,

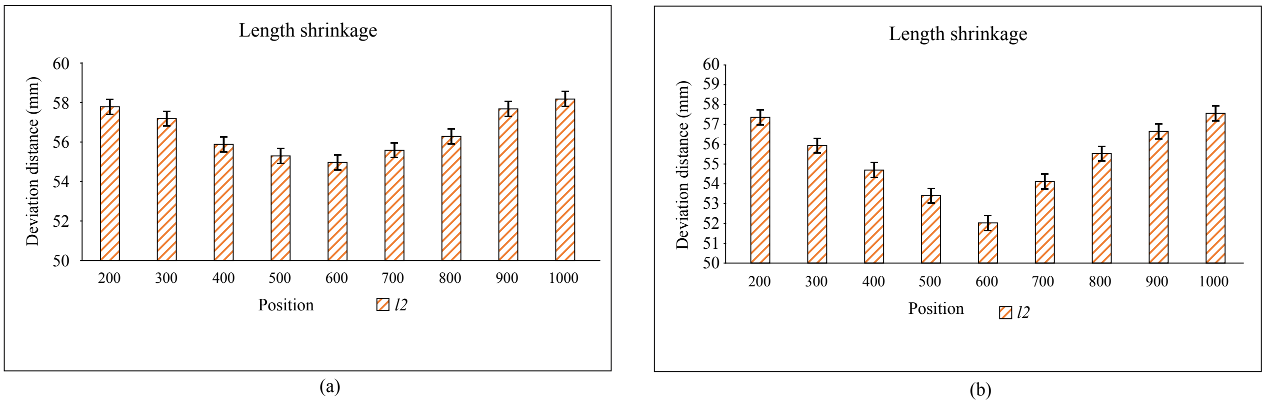

Figure 5 The longitudinal shrinkage of sample 3A1 (a) and sample 7B3 (b)

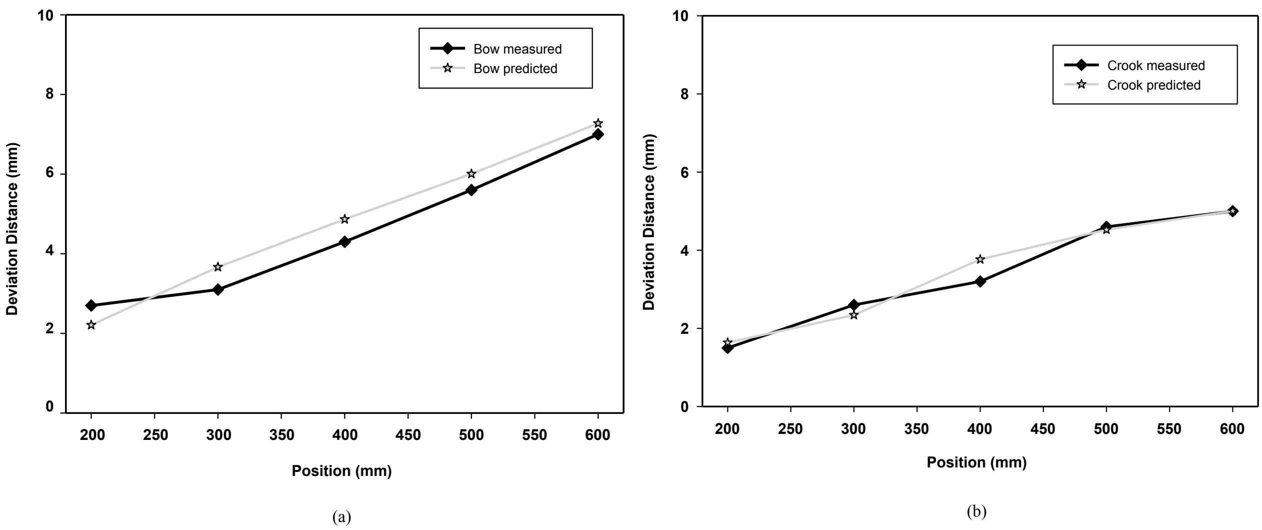

Figure 6 Measured and predicted values of (a) bow (sample 7B3) and (b) crook (sample 3A1)

Table 4 The longitudinal shrinkage coefficients for the samples from each run

Run no.	Mean	Standard deviation
1	0.1265	0.0467
2	0.1751	0.0681
3	0.1194	0.0412
4	0.1115	0.0559
5	0.1020	0.0448
6	0.1090	0.0299
7	0.1405	0.0523
8	0.2067	0.0847
9	0.1484	0.0606

Table 5 Average mechanical properties of rubberwood dried at different temperatures

Property	Drying temperature		
	80 °C	100 °C	120 °C
Compressive stress (MPa)			
Parallel to grain	40.21 ± 0.88	38.16 ± 4.10	40.75 ± 5.98
Perpendicular to grain	22.01 ± 0.93	23.58 ± 1.06	26.8 ± 5.95
Static bending (MPa)			
Modulus of rupture (MOR)	81.85 ± 6.43	85.32 ± 7.51	81.12 ± 16.05
Modulus of elasticity (MOE)	7838.35 ± 1140.21	8679.38 ± 790.22	8012.84 ± 2055.74

(a) (b)

Figure 7 Compression testing parallel to the grain (a) and measuring a sample (b)

the test results of mechanical properties after rubberwood drying were suitable for to be used in the wood processing steps.

Colour measurement of the samples

The samples were compared with the wood standards of a local factory as shown in Figure 8. The development of discoloration was rapid at high temperatures but became slower and more erratic at the lower temperatures. Table 6 provided the total change in the surface colour of the wood (ΔE). The results indicated that the ΔE increased with temperature and with duration of the treatment. The heat-treated wood had uniform colour throughout as the

Figure 8 The samples for colour measurement

Table 6 Development of colour coordinates of rubberwood during kiln drying

No.	Drying temperature (°C)	Colour development			
		Δ*L*	Δ*a*	Δ*b*	Δ*E*
1	80	-1.69	0.43	-0.17	1.75
2	100	-4.1	1.36	1.63	4.62
3	120	-7.13	2.56	2.04	7.85
4	80	1.69	-1.24	0.44	2.14
5	100	-4.18	2.9	0.37	5.10
6	120	-8.37	2.77	1.02	8.88
7	80	-2.84	1.86	-0.14	3.40
8	100	-3.02	0.34	1.72	3.49
9	120	-8.61	2.87	0.28	9.08

Δ = Differential between total discoloration based on average in manufacturing after drying of rubberwood and colour development conducted on the laboratory scale based on percent of average drying time; Δ*L* = the lightness difference, Δ*a*= the red-green difference, Δ*b* = blue-yellow difference, Δ*E*= the colour difference

similar trends were also observed in other studies (Ratnasingam & Grohmann 2014). The variability in discoloration indicated that the properties of rubberwood had stronger influence on discoloration at lower temperatures than at high temperatures due to the temperature-dependent kinetics were much slower.

CONCLUSIONS

The current study managed to present measurements of the distorted geometry along the length of 81 rubberwood samples. Wood drying stress was high at 100 °C and 120 °C due to the sudden decreased in the internal moisture content of the wood. Wood distortion during drying occurred at the moisture content above 30%. The longitudinal shrinkage in the samples was observed when the moisture content changed from 16% to 8%. A model was developed to predict the changes in magnitudes of bow and crook between the two moisture contents. The model showed that the changes in bow and crook of the samples explained the variation in the longitudinal shrinkage coefficient over the cross-section and along the lumber. Using the variation in the longitudinal shrinkage to model bow and crook had shown significantly good accuracy. Therefore, these findings could further contribute and be implemented to ensure the good mechanical properties of wood.

ACKNOWLEDGEMENTS

The authors were grateful for the financial support from the Prince of Songkla Graduate Studies Grant and Rubberwood Technology and Management Research Group (ENG-54-27-11-0137-S). The authors also thanked A.P.K. Furnishing Parawood Co. Ltd for supplying the samples

REFERENCES

Altgen M & Militz H. 2016. Influence of process conditions on hygroscopicity and mechanical properties of European beech thermally modified in a high-pressure reactor system. *Holzforschung* 70: 971–979.

ASTM D143-14. 2014. *Standard Test Methods for Small Clear Specimens of Timber.* ASTM International, West Conshohocken, Pennsylvania.

Bao F & Liu S. 2007. Modelling the relationships between wood properties and quality of veneer and plywood of Chinese plantation poplars. *Wood and Fiber Science* 33: 264–274.

Cáceres CB, Hernández RE & Fortin Y. 2018. Shrinkage variation in Japanese larch (*Larix kaempferi*, [Lamb.] Carr.) progenies/provenances trials in Eastern Canada. *Wood Material Science & Engineering* 13: 97–103.

Calonego FW, Severo ETD & Ballarin AW. 2012. Physical and mechanical properties of thermally modified wood from *E. grandis*. *European Journal of Wood and Wood Products* 70 :453–460.

Cermak P & Trcala M. 2012. Influence of uncertainty in diffusion coefficients on moisture field during wood drying. *International Journal of Heat and Mass Transfer* 55: 7709–7717.

Chang YS, Han Y, Shin HK et al. 2020. Evaluation of drying and anatomical characteristics of Mongolian oak lumber by kiln drying with respect to storage time after sawing. *European Journal of Wood and Wood Products* 78: 1017–1022.

Gnanaharan R & Dhamodaran TK. 1993. Mechanical properties of rubberwood from a 35-year-old plantation in Central Kerala, India. *Journal of Tropical Forest Science* 6: 136–140.

González-Peña MM & Hale MDC. 2009. Colour in thermally modified wood of beech, Norway spruce and Scots pine. Part 2: Property predictions from colour changes. *Holzforschung* 63: 394–401.

Hadi YS, Massijaya MY, Nandika D et al. 2020. Colour change and termite resistance of fast-growing tropical woods treated with kesambi (*Schleichera oleosa*) smoke. *Journal of Wood Science* 66: 61.

Johansson M. 2003. Prediction of bow and crook in timber studs based on variation in longitudinal shrinkage. *Wood and Fiber Science* 35: 445–455

Kaung MT & Thanate R. 2020. Coefficient of thermal expansion of rubberwood (*Hevea brasiliensis*) in convective drying process. *Journal of Tropical Forest Science* 32: 72–82.

Khamtree S, Ratanawilai T & Nuntadusit C. 2019. An approach for indirect monitoring of moisture content in rubberwood (*Hevea brasiliensis*) during hot air drying. Drying Technology 37: 2116–2125.

Khamtree S, Ratanawilai T, Nuntadusit C et al. 2021. Experimental study and numerical modeling of heat and mass transfer in rubberwood during kiln drying. *Heat and Mass Transfer* 57: 453–464.

Kliger R, Johansson M, Perstorper M et al. 2003. Distortion of Norway spruce timber. *European Journal of Wood and Wood Products* 61: 241–250.

Kubojima Y, Kobayashi I, Yoshida T et al. 2013. Twisting force during drying of wood. *European Journal of Wood and Wood Products* 71: 689–695.

Lazarescu C, Avramidis S & Oliveira L. 2009. Modeling shrinkage response to tensile stresses in wood drying: I. shrinkage-moisture interaction in stress-free specimens. *Drying Technology* 27: 1183–1191.

Lazarescu C, Avramidis S & Oliveira L. 2010. Modelling shrinkage response to tensile stresses in wood drying II. stress-shrinkage correlation in restrained specimens. *Drying Technology* 28: 186–192.

Matan N & Kyokong B. 2003.) Effect of moisture content on some physical and mechanical properties of juvenile rubberwood (*Hevea brasiliensis* Muell. Arg.). *Songklanakarin Journal of Science and Technology* 25: 327–340.

Monteiro SRS, Martins C, Dias AMPG et al. 2020. Mechanical performance of glulam products made with Portuguese poplar. *European Journal of Wood and Wood Products* 78: 1007–1015.

Ormarsson S & Cown D. 2005. Moisture-related distortion of timber boards of radiata pine: comparison with Norway spruce. *Wood and Fiber Science* 37: 424–436.

Peng M, Kershaw JA, Chui YH et al. 2013. Modelling of tangential, radial, and longitudinal shrinkage after drying in jack pine and white spruce. *Canadian Journal of Forest Research* 43: 742–749.

Ratanawilai T, Nuntadusit C & Promtong N. 2015. Drying characteristics of rubberwood by impinging hot-air and microwave heating. *Wood Research* 60: 59–70.

Ratnasingam J & Grohmann R. 2014. Color development in rubberwood (*Hevea brasiliensis*) during kiln drying. *European Journal of Wood and Wood Products* 72: 555–557.

Roblot G, Coudegnat D, Bleron L et al. 2008. Evaluation of the visual stress grading standard on French Spruce (*Picea excelsa*) and Douglas-fir (*Pseudotsuga menziesii*) sawn timber. *Annals of Forest Science* 65: 812.

Ross RJ & Service FPLUF. 2010. *Wood Handbook: Wood as An Engineering Material.* General Technical Report FPL- GTR-190, 2010: 509 p 1 v 190. USDA Forest Service, Forest Products Laboratory, United States.

Sik HS, Choo KT, Sarani Z et al. 2009. Influence of drying temperature on the physical and mechanical properties of rubberwood. *Journal of Tropical Forest Science* 21: 181–189.

Sik HS, Choo KT, Zakaria S et al. 2010. Dimensional stability of high temperature-dried rubberwood solid lumber at two equilibrium moisture content conditions. *Drying Technology* 28: 1083–1090.

Simpson WT. 1991. *Dry Kiln Operator's Manual*. Forest Products Laboratory, U.S. Dept. of Agriculture, Forest Service, Wisconsin, United States.

Staff BSI & Institution BS. 1957. *Methods of Testing Small Clear Specimens of Timber*. British Standards Institution, London.

Tiryaki S & Aydin A. 2014. An artificial neural network model for predicting compression strength of heat-treated woods and comparison with a multiple linear regression model. *Construction and Building Materials* 62: 102–108.

Walker JCF. 2006. *Primary Wood Processing: Principles and Practice*, 2nd edition. Springer, Dordrecht, The Netherlands.

Yamsaengsung R & Tabtiang S. 2011. Hybrid drying of rubberwood using superheated steam and hot air in a pilot-scale. *Drying Technology* 29: 1170–1178.